Photoinduced Metallic State Mediated by Spin-Charge Separation in a One-Dimensional Organic Mott Insulator

H. Okamoto,[1,2,3] H. Matsuzaki,[1,3] T. Wakabayashi,[1] Y. Takahashi,[2] and T. Hasegawa[2]

[1]*Department of Advanced Materials Science, University of Tokyo, Kashiwa, 277-8561, Japan*

[2]*Correlated Electron Research Center (CERC), National Institute of Advanced Industrial Science and Technology (AIST), Tsukuba, 305-8562, Japan*

[3]*CREST, JST, Kawaguchi 332-0012, Japan*

(Received 7 August 2006; published 16 January 2007)

Charge dynamics in a one-dimensional (1D) Mott insulator was investigated by fs pump-probe reflection spectroscopy on an organic charge-transfer compound, bis(ethylenedithio)tetrathiafulvalene-difluorotetracyanoquinodimethane (ET-F_2TCNQ). The analyses of the transient reflectivity changes demonstrate that low-energy spectral weight induced by photocarrier doping is concentrated on a Drude component being independent of the doping density, and midgap state is never formed. Such phenomena can be explained by the concept of spin-charge separation characteristic of 1D correlated electron systems.

DOI: 10.1103/PhysRevLett.98.037401 PACS numbers: 78.47.+p, 71.30.+h, 78.20.Ci, 78.40.Me

The electronic structures of Mott insulators exhibit large variations with respect to carrier doping [1]. A typical example is the insulator-metal transition in the perovskite-type cuprates due to the carrier doping to the CuO_2 layers [2,3]. As demonstrated in underdoped cuprates such as $La_{2-x}Sr_xCuO_4$ ($Nd_{2-x}Ce_xCuO_4$) with $x < 0.05$, the motion of holes (electrons) disrupts the antiferromagnetic spin background through the coupling of charge and spin degrees of freedoms, resulting in a midgap absorption (the incoherent part). Further carrier doping gives rise to the metallic state, although the Drude weight is small as compared to the midgap absorption [3]. Two-dimensional (2D) and 3D Mott insulators of other 3*d* transition metal oxides also exhibits similar doping dependence [1].

Previous theoretical studies suggested that in half-filled 1D Mott insulators, the spectral weight of the gap-transition is transferred to the Drude component by the carrier doping, irrespective of carrier density [4,5]. Such a feature originates from the spin-charge separation characteristic of 1D strongly correlated electron systems (SCESs) [5,6] and is in contrast with 2D and 3D SCESs [7–9]. However, 1D SCESs in which the amount of carriers can be widely controlled through chemical modifications have not been reported. Photoirradiation is another effective method for the control of the carrier density [10–14]. Photocarrier doping on 1D Mott insulators was studied in the Br-bridged Ni-chain compound [12]. The results revealed that for the small carrier doping with an excitation less than 0.05 photon (ph.)/Ni, a midgap absorption is formed. This result indicates that carriers are localized due to electron-lattice (*e*-*l*) interaction [12]. Further carrier doping with an excitation larger than 0.1 ph./Ni induces a metallic state. From the experimental viewpoint, therefore, charge dynamics and metallic behavior for the small carrier density in 1D SCESs have not been clarified.

In this Letter, we report the first demonstration of the photoinduced metallic states irrespective of the photocarrier density in a 1D Mott insulator using the fs pump-probe (PP) reflection spectroscopy technique on an organic charge-transfer (CT) compound, bis(ethylenedithio)-tetrathiafulvalene-difluorotetracyanoquinodimethane (ET-F_2TCNQ). Photoinduced reflectivity changes exhibit no midgap absorption, but exhibit a Drude response, even for the small excitation-density (0.003 ph./site). In ET-F_2TCNQ, the suppression of the *e*-*l* interaction enables us to observe clearly metallic states mediated by the spin-charge separation. For a larger excitation density (0.095 ph./site), the decay time of the metallic state decreases significantly to less than the time resolution ($\sim$ 180 fs), attributable to the strong electron-electron (*e*-*e*) scattering. The dynamics of the photoinduced metallic states will be discussed with respect to the analyses of transient reflectivity spectra.

ET-F_2TCNQ, is a segregate-stacked CT compound [15], the crystal structure of which is presented in the inset of Fig. 1(b); each acceptor (*A*) molecule (F_2TCNQ) is isolated from neighboring *A* molecules and donor (*D*) molecules (ET). The CT interaction is effective only between neighboring ETs. An electron is transferred from an ET to an F_2TCNQ, such that half-filled ET chains dominate its electronic properties. The electrons are localized at each site [Fig. 1(c)-i] because of large *U* on ET that overcomes the electron transfer energy, *t*, between the neighboring ETs. Thus, the compound becomes a Mott insulator. Organic compounds with half-filled 1D SCESs sometimes exhibit molecular dimerizations due to the spin-Peierls (SP) mechanism [16,17], which is a consequence of the strong spin-lattice (*s*-*l*) interaction. Exceptionally, ET-F_2TCNQ exhibits no SP dimerization even at low temperatures, but exhibits an antiferromagnetic transition at 30 K [15], indicating that *s*-*l* interaction is very weak.

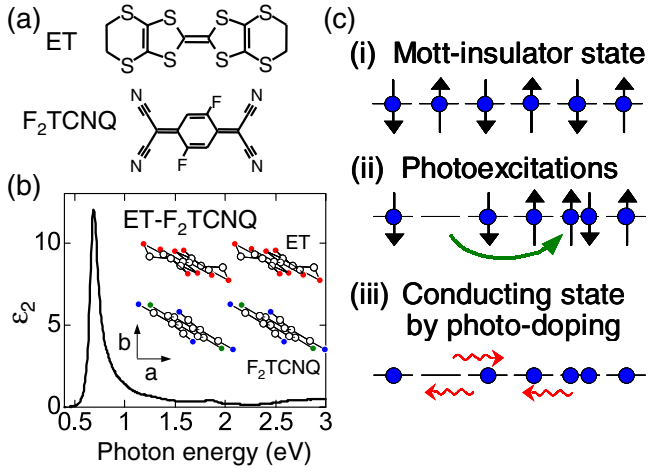

FIG. 1 (color online). (a) The molecular structures of ET and F_2TCNQ. (b) The ε_2 spectrum for $E \parallel \mathbf{a}$ (the stacking axis) of ET-F_2TCNQ; the inset is a view of the crystal structure along the normal to the ab plane. (c) Schematic view of (i) Mott insulator state of the ET^+ chain, (ii) photocarrier doping, and (iii) photo-induced conducting state.

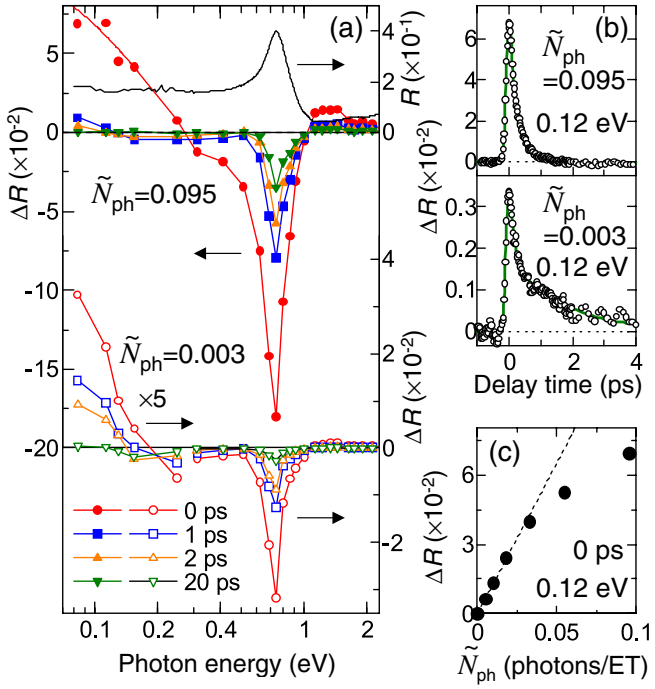

FIG. 2 (color online). (a) Photoinduced reflectivity changes (ΔR) of ET-F_2TCNQ for the 1.55 eV pump and the photon densities of $\tilde{N}_{ph} = 0.003$ and 0.095 ph./ET. The pump and probe lights are polarized parallel to **a**. The upper solid line represents the polarized R spectrum along **a**. (b) Experimental (circles) and calculated (solid lines) time profiles of ΔR at 0.12 eV. (c) $\tilde{N}_{ph}$ dependence of ΔR at 0.12 eV and at $t_d =$ 0 ps. The broken line shows a linear relation.

The ET chain is formed from the side-by-side coupling between neighboring ETs. Such a molecular arrangement is known to suppress e-l interactions as well as s-l interactions [15], resulting in negligible polaronic effects on carriers. Therefore, ET-F_2TCNQ is a good candidate for the study of the charge dynamics characteristic of 1D SCESs.

Single crystals of ET-F_2TCNQ were grown from recrystalization as outlined in a previous report [15]. In the fs PP reflection spectroscopy, the laser source is a Ti:Al_2O_3 regenerative amplifier. The wavelength, the pulse width, and the repetition frequency of its output are 800 nm (1.55 eV), 130 fs, and 1 kHz, respectively. The output was used for the pump light and for the excitation of an optical parametric amplifier from which the probe light (0.08 to 2.5 eV, 130 fs) was obtained.

Figure 1(b) is the spectrum of the imaginary part of the dielectric constant ε_2 for the electric filed of light (E) parallel to the ET stacking axis **a** ($E \parallel \mathbf{a}$), obtained from the polarized reflectivity (R) spectrum using the Kramers-Kronig transformation (KKT), as presented in the upper part of Fig. 2(a). A clear peak at ~0.7 eV corresponds to the Mott-gap transition expressed as $(ET^+, ET^+) \rightarrow (ET^{+2}, ET^0)$ [Fig. 1(c)-(ii)] [15]. No structures are observed for $E \parallel \mathbf{b}$ and $E \parallel \mathbf{c}$ in this region. This indicates the strong 1D nature of the ET chain.

Photoinduced R change (ΔR) spectra for the 1.55 eV pump are presented in Fig. 2(a). The electric fields of both the pump and probe lights are parallel to **a**. The lower (upper) spectra are the results for the weak (strong) excitation with $\tilde{N}_{ph} = 0.003$ ($\tilde{N}_{ph} = 0.095$) ph./ET. Here, $\tilde{N}_{ph}$ is defined as the averaged photon density within the absorption depth l_p (~ 5800 Å) of the pump light, expressed by $(1 - R_p)(1 - 1/e)N_{ex}/l_p$, and R_p (~ 0.053) is the reflection loss and N_{ex} is the areal excitation photon density. l_p is obtained from KKT of the R spectrum in Fig. 2(a). In both the weak and strong excitations, R decreases in the gap-transition region and increases in the IR region, indicating that the spectral weight of the gap transition is transferred to the inner-gap region. ΔR monotonously increases for a decreasing energy, suggesting the formation of a conducting state [Fig. 1(c)-(iii)]. The energy position at which ΔR crosses zero for $\tilde{N}_{ph} =$ 0.095 ph./ET is higher than that for $\tilde{N}_{ph} = 0.003$ ph./ET. Such an energy shift indicates that the response is not due to a midgap state but to a Drude-type metallic state.

To characterize the photoinduced metallic state, we analyzed ΔR spectra using a simple Drude model. When a single crystal is irradiated with light, the amount of absorbed photons and the number of generated carriers decreases as the distance z from the crystal surface is increased, depending on l_p, as illustrated in Fig. 3(a). To take these effects into account, we assume that the carrier density $N_c(z)$ is expressed by $N_c(z) = N_c(0) \exp(-z/l_p)$, where $N_c(0)$ is the carrier density at the surface. We also assume that the effective masses of electron and hole carriers (m_e^* and m_h^*) are equal to the free electron mass m_0. On the basis of these assumptions, the dielectric constant can be expressed as follows [18],

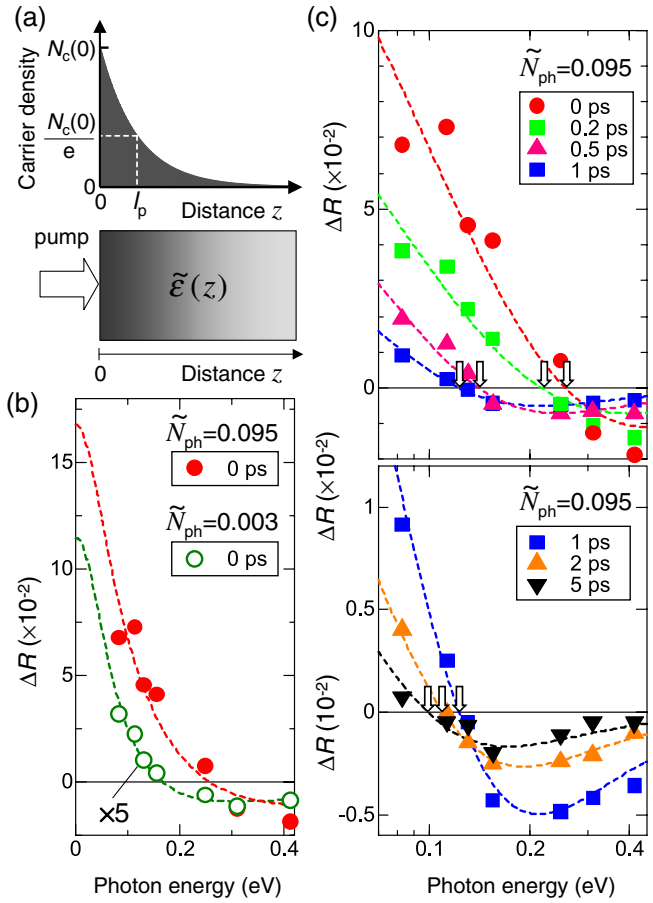

FIG. 3 (color online). (a) Illustrations of the carrier density N_c as a function of the distance z from the surface. (b) Experimental (circles) and calculated (broken lines) ΔR spectra at $t_d = 0$ ps for $\tilde{N}_{ph} = 0.003$ and 0.095 ph./ET. (c) Experimental (solid marks) and calculated (broken lines) ΔR spectra at various t_d for $\tilde{N}_{ph} = 0.095$ ph./ET. The arrows indicate the energy positions for $\Delta R = 0$.

$$\varepsilon(z) = \varepsilon_s - \frac{e^2}{\varepsilon_0 m_0}\frac{1}{\omega^2 + \gamma^2}\left(1 - i\frac{\gamma}{\omega}\right)N_c(z) \qquad (1)$$

where γ is the damping constant. $\varepsilon_s (= 5.5)$ is the static dielectric constant obtained from KKT of the R spectrum, and $N_c(0)$ is related to the averaged carrier density $\tilde{N}_c$ within l_p as $\tilde{N}_c = (1 - 1/e)N_c(0)$. From Eq. (1), we can calculate ΔR using the two parameters $\tilde{N}_c$ and γ. As plotted in Fig. 3(b), the analytical results (broken lines) are in agreement with the experimentally determined ΔR spectra (circles) with the parameters of $\gamma = 0.34$ eV and $\tilde{N}_c = 0.005/\text{ET}$ for $\tilde{N}_{ph} = 0.003$ ph./ET and $\gamma = 0.47$ eV and $\tilde{N}_c = 0.059/\text{ET}$ for $\tilde{N}_{ph} = 0.095$ ph./ET. This demonstrates that the formation of the metallic state is independent of the carrier density.

The dynamical processes of the photoinduced metallic state were also investigated. Time profiles of ΔR at 0.12 eV are presented in Fig. 2(b). It is found that the response time is very short, that is, ΔR recovers within 4 ps for $\tilde{N}_{ph} = 0.003$ ph./ET and within 1 ps for $\tilde{N}_{ph} = 0.095$ ph./ET. The decay time of ΔR seems to be comparable to the pulse width (~ 130 fs). Thus, we analyzed the time profiles using temporal Gaussian profiles of the pump and probe pulses, and the corresponding convolution integrals. Here, we adopt two exponential functions as follows,

$$\frac{\Delta R(t_d)}{R} \propto \sum_{i=1,2} A_i \int_{-\infty}^{t_d} \exp\left(\frac{t' - t_d}{\tau_i} - \frac{t'^2}{\tau_0^2}\right)dt', \left(\sum_i A_i = 1\right) \qquad (2)$$

τ_0, the parameter associated with the pulse duration, is set to be 140 fs. τ_i, and A_i ($i = 1, 2$) are the decay time and the relative weight of each exponential component, respectively. By using $\tau_1 = 114$ fs ($A_1 = 0.72$) and $\tau_2 = 1.72$ ps ($A_2 = 0.28$) for $\tilde{N}_{ph} = 0.003$ ph./ET and $\tau_1 = 27$ fs ($A_1 = 0.81$) and $\tau_2 = 320$ fs ($A_2 = 0.19$) for $\tilde{N}_{ph} = 0.095$ ph./ET, the experimental time profiles were reproduced well as shown by the solid lines in Fig. 2(b).

The decay of ΔR for $\tilde{N}_{ph} = 0.003$ ph./ET is much longer than that for $\tilde{N}_{ph} = 0.095$ ph./ET. This may be explained by the fact that carrier recombination rate decreases as the carrier density is decreased. To confirm this, we focus on the time dependence of ΔR spectra in the IR region for $\tilde{N}_{ph} = 0.095$ ph./ET shown in Fig. 3(c). As indicated by the arrows, the energy at which ΔR is zero decreases with time. When we assume a Drude model, the crossing position is a rough measure for the plasma frequency. That is, the decrease of the energy at which ΔR is zero is directly related to the decrease in the carrier density. In fact, the ΔR spectra for $t_d > 0$ ps is reproduced using Eq. (1), as indicated by the broken lines in Fig. 3(c). The fitting parameters $\tilde{N}_c$ (triangles) and γ (squares) were plotted in Fig. 4, with the experimental (open circles) and calculated (solid line) time profiles of ΔR.

As in Fig. 4, γ (the mean free time $\tau = 1/\gamma$) changes from 0.5 eV (8 fs) to 0.12 eV (30 fs) with time. A sharp decrease of γ, up to $t_d \sim 0.5$ ps, corresponds to a steep decrease of $\tilde{N}_c$, attributed to the suppression of the e-e scattering because of the decrease in the carrier density. In this case, τ should be smaller than the decay time of $\tilde{N}_c$. From the analyses presented above, it is possible to express the inequality $\tau < \tau_1$. To be exact, γ will be a function of z when γ depends on the carrier density. Our spectral analyses neglect this effect. Thus, we should consider γ as an averaged value. Moreover, it is natural to consider that the decay rate of ΔR changes with t_d, depending of the carrier density. Therefore, our analyses using Eq. (1) are not perfect but rather formal; $\tau < \tau_1$ is, however, consistent supporting our interpretations.

It is valuable to comment on the reflectivity values for the photoinduced metallic state. The broken lines in Fig. 3(b) indicate that $R + \Delta R$ at 0 eV was 0.21 for $\tilde{N}_{ph} = 0.003$ ph./ET and 0.35 for $\tilde{N}_{ph} = 0.095$ ph./ET, much smaller than 1. When the carrier density is inhomogeneous, the reflectivity never reaches 1 even when assuming a

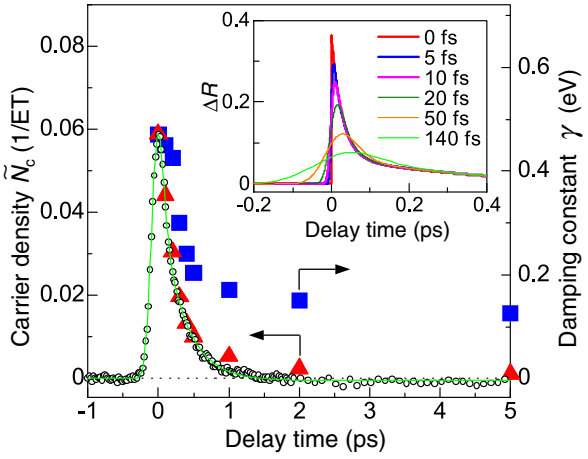

FIG. 4 (color online). Time dependence of the carrier density $\tilde{N}_c$ (triangles) and the damping constant γ (squares) for $\tilde{N}_{\mathrm{ph}} = 0.095$ ph./ET. The open circles are the time profiles of ΔR at 0.12 eV, and the solid line is a fitting curve (see text). The inset is the simulated time profiles of ΔR for various pulse widths (τ_0).

Drude response. Furthermore, the decay time of carriers, τ_1, is smaller than the pulse width. In this case, ΔR at $t_d = 0$ ps is affected by the relaxation processes during the pulse. The magnitude of ΔR, therefore, should be enhanced if instantaneous photocarrier doping is performed. We simulated time profiles of ΔR at 0.12 eV for different values of τ_0 in Eq. (2) with the parameters of $\tau_1 = 27$ fs ($A_1 = 0.81$) and $\tau_2 = 320$ fs ($A_2 = 0.19$), presented in the inset of Fig. 4. When we assume $\tau_0 = 0$ fs, that is, the excitation by a δ-function pulse, the magnitude of ΔR is 3 times higher than that for $\tau_0 = 140$ fs, and thus, $R + \Delta R$ exceeds 0.5 at 0.12 eV.

We can now discuss the nature of the observed metallic states. For $\tilde{N}_{\mathrm{ph}} = 0.003$ ph./ET, ΔR at $t_d = 0$ ps is only -0.03 at 0.7 eV; thus, the original peak due to the Mott-gap transition is not so changed. It suggests that most of the electrons are still localized on each site. For $\tilde{N}_{\mathrm{ph}} = 0.095$ ph./ET, ΔR at $t_d = 0$ ps is ~ -0.2 at 0.7 eV where the original peak almost disappears, so that the Mott gap is collapsed. Such a change in the increase of the carrier density occurs continuously since the excitation-density dependence of ΔR at 0.12 eV in Fig. 2(c), which is a crude measure of the Drude weight, does not exhibit any symptoms of critical behaviors. This suggests that the photo-induced insulator-metal transition in ET-F_2TCNQ is not a first-order transition but a continuous one. As reported in the theoretical studies, for the carrier doping of a half-filed 1D Mott insulator with a finite U, all of the spectral weight removed from the gap transition is transferred to the Drude component, irrespective of the amounts of carriers [4,5]. That is due to the spin-charge separation [5,6]. The theoretical studies also indicated that for the half-filled case, the Drude weight starts to increase continuously from zero and gradually enhances with the carrier density [5]. All the results for ET-F_2TCNQ are fairly consistent with these theoretical predictions.

To obtain information on the pump-energy dependence of the response, the ΔR spectrum was also measured under a resonant excitation of the gap transition. The results showed that the insulator-metal transition occurred and that the spectral shape of ΔR and its time dependence were almost equal to those obtained for the 1.55-eV pump. When there is a strong excitonic effect, excitons will produce an optical response different from the Drude response. Thus, our results suggest that the excitonic effect is very small in ET-F_2TCNQ.

So far, the photocarrier doping on 1D Mott insulators was investigated in the Br-bridged Ni-chain compound, $[\mathrm{Ni(chxn)_2Br}]\mathrm{Br_2}$ (chxn = cyclohexanediamine) [12,14]. Through an excitation of less than 0.05 ph./Ni, a midgap absorption due to small polarons was observed. Other 1D Mott insulators such as Sr_2CuO_3 [19] and an SP system of K-TCNQ [20] also exhibited similar midgap absorptions. In contrast, in ET-F_2TCNQ, the Drude-type metallic state was formed even for a small carrier density. Thus, the result for ET-F_2TCNQ is the first unambiguous demonstration of the metallic state caused by the decoupling of spin and charge degrees of freedoms.

In summary, the suppression of the electron-lattice interaction in ET-F_2TCNQ enables us to observe charge dynamics for photocarrier doping in a 1D Mott insulator. A weak photoexcitation can induce a metallic state. That can be explained by the concept of the spin-charge separation. For a larger photoexcitation, the decay time of the metallic state is significantly lower, suggesting that electron-electron scattering plays an important role.

[1] For a review, M. Imada *et al.*, Rev. Mod. Phys. **70**, 1039 (1998).
[2] S. L. Cooper *et al.*, Phys. Rev. B **41**, 11 605 (1990).
[3] S. Uchida *et al.*, Phys. Rev. B **43**, 7942 (1991).
[4] R. M. Fye *et al.*, Phys. Rev. B **44**, 6909 (1991).
[5] H. Eskes and A. M. Oles, Phys. Rev. Lett. **73**, 1279 (1994).
[6] M. Ogata and H. Shiba, Phys. Rev. B **41**, 2326 (1990).
[7] E. Dagotto *et al.*, Phys. Rev. B **45**, 10 741 (1992).
[8] H. Eskes *et al.*, Phys. Rev. B **50**, 17 980 (1994).
[9] T. Tohyama *et al.*, J. Phys. Soc. Jpn. **69**, 9 (2000).
[10] G. Yu *et al.*, Phys. Rev. Lett. **67**, 2581 (1991).
[11] F. O. Karutz *et al.*, Phys. Rev. Lett. **81**, 140 (1998).
[12] S. Iwai *et al.*, Phys. Rev. Lett. **91**, 057401 (2003).
[13] A. Cavalleri *et al.*, Phys. Rev. B **70**, 161102(R) (2004).
[14] S. Iwai and H. Okamoto, J. Phys. Soc. Jpn. **75**, 011007 (2006).
[15] T. Hasegawa *et al.*, Solid State Commun. **103**, 489 (1997).
[16] J. B. Torrance, in *Low-dimentional Conductors and Superconductors*, edited by D. Jerome and L. G. Caron, NATO Advanced Study Institutes, Ser. B., Vol. 155 (Plenum Press, New York, 1987).
[17] K. Yonemitsu and M. Imada, Phys. Rev. B **54**, 2410 (1996).
[18] J. Y. Vinet *et al.*, Solid State Commun. **51**, 171 (1984).
[19] H. Okamoto *et al.* (unpublished).
[20] H. Okamoto *et al.*, Phys. Rev. Lett. **96**, 037405 (2006).